Solution Structure of Human Survivin and Its Binding Interface with Smac/Diablo‡

Chaohong Sun, David Nettesheim, Zhihong Liu, and Edward T. Olejniczak*

Global Pharmaceutical Discovery Division, Abbott Laboratories, Abbott Park, Illinois 60064

Received July 13, 2004; Revised Manuscript Received October 11, 2004

ABSTRACT: NMR studies of the antiapoptotic protein survivin have been used to determine the homodimer interface of the protein in solution and to identify residues of the protein that interact with Smac/Diablo. In solution, survivin(1−120) forms a bow-tie-shaped dimer whose interface is composed of its N-terminal residues as well as residues connecting its BIR domain to the C-terminal α helix. The solution structure resolves the controversy regarding the two possible dimer interfaces for survivin observed in X-ray crystal structures. The structural basis for the interaction between survivin and Smac/Diablo was also investigated. When Smac/Diablo or N-terminal Smac/Diablo peptide analogues are added to a solution of survivin, specific residues near α4 and β3 are perturbed. NMR experiments indicate that the peptides bind across the third β-strand of survivin in a manner similar to the way Smac/Diablo peptides bind to the BIR3 domain of X-linked IAP (XIAP).

Survivin is selectively overexpressed in most human cancers but not in normal tissues (*1*, *2*). It is a member of the inhibitor-of-apoptosis (IAP) family of proteins. IAP proteins play an important role in apoptosis by being endogenous inhibitors of caspases (*3*). This inhibition can be relieved by a mitochondrial protein, Smac/Diablo, which directly binds to IAPs and thus suppresses their function (*4*, *5*). Survivin has been reported to exhibit anti-apoptotic activity; however, its mechanism is still not clear (*1*, *2*, *6*−*8*). One suggestion is that it does not bind caspases directly, but instead exerts an anti-apoptotic effect by binding to Smac/Diablo and neutralizing the Smac/Diablo effect on other IAPs (*8*). Survivin may also be a member of another distinct group of BIR[1] domain containing proteins that are found to localize to the mitotic spindle (*9*−*11*). In *Caenorhabditis elegans*, the survivin-like BIR1 protein localizes the aurora-like kinase AIR-2 to the chromosome. Recent studies indicate that human survivin interacts with aurora-B kinase, stimulates its activity, and helps target aurora-B kinase to its substrates during the cell cycle (*12*).

Structurally, the survivin monomer (1−142) contains a zinc-binding fold similar to that found in the XIAP BIR2, BIR3 domain (*13*, *14*), but it lacks the RING finger motif found in XIAP. Instead, survivin contains a long amphipathic helix C-terminal to the BIR domain (*15*−*17*). On the basis of both ultracentrifugation and gel filtration chromatography, survivin behaves like a homodimer in solution. However, two different crystal packing modes were found for the mouse and human survivin proteins (*15*−*17*). This leads to two very different models for the proposed dimer interface (*18*). Mutagenesis has been done on the basis of the two different dimer models, but these data have been unable to unambiguously resolve the relevant dimer in solution.

In this study, we describe the solution structure of human survivin as determined by NMR spectroscopy. These data unambiguously define the dimer interface found in solution. We also describe our binding studies of human survivin and Smac/Diablo. Residue-specific resonance perturbations are observed that help define the interface between the two proteins. N-terminal Smac/Diablo-like peptides were tested and found to perturb the same resonances as mature Smac/Diablo. NMR studies on an N-terminal Smac/Diablo-like peptide were used to understand how this peptide binds to survivin.

EXPERIMENTAL PROCEDURES

Protein Preparation. Survivin(1−120) with a N-terminal 6× histidine tag was prepared by expressing the protein in *Escherichia coli* BL21(DE3) and grown on M9 media. Uniformly ^{15}N-labeled; uniformly ^{15}N,^{13}C-labeled; and uniformly ^{15}N,^{13}C-labeled, 75% ^{2}H samples were prepared with media containing either $^{15}NH_4Cl$; $^{15}NH_4Cl$ plus [U-^{13}C]glucose; or $^{15}NH_4Cl$, [U-^{13}C]glucose, and 75% $^{2}H_2O$, respectively. Soluble protein was purified by Ni^{2+}-affinity chromatography. The histidine tag was cleaved off with thrombin and removed with a Ni^{2+}-affinity column. A metal-chelating column was used to remove any trace amount of Ni.

To determine intermonomer contacts, we prepared a survivin sample that contained dimers consisting of an isotopically labeled (^{15}N,^{13}C) and an unlabeled monomer. The sample was generated by mixing a uniformly labeled

‡ The average minimized coordinates for the survivin dimer structure have been deposited with the Protein Data Bank (PDB accession code 1XOX). The assignments for survivin have been deposited with the BioMagRes database (ID 6342).

* To whom correspondence should be addressed. Mailing address: Abbott Laboratories, 100 Abbott Park Rd., R46Y, AP10, Abbott Park, IL 60064-6098. Phone: (847) 937-0298. Fax: (847) 938-2478. E-mail: edward.olejniczak@abbott.com.

[1] Abbreviations: NMR, nuclear magnetic resonance; NOE, nuclear Overhauser effect; rmsd, root-mean-squared deviation; SAR, structure−activity relationships; BIR, baculoviral inhibitory repeat; ABU, α-aminobutyric acid; Aib, α-aminoisobutyric acid, Tle, *tert*-leucine; Aze, azetidine-2-carboxylic acid; Cha, cyclohexylalanine; Cl-Phe, 4-chlorophenylalanine; Hyp, (4*R*)-4-hydroxyproline; 1-Nal, 1-naphthylalanine; 2-Nal, 2-naphthylalanine; Nle, norleucine; Pip, pipecolic acid; Sar, sarcosine.

10.1021/bi0485171 CCC: $30.25
Published on Web 12/08/2004

Table 1: Structural Statistics and Root-Mean-Square Deviations for 10 Dimer Structures of Survivin(1−120)

	$\langle SA \rangle^a$	$\overline{\langle SA \rangle}_{min}$
rmsd from experimental distance restraints (Å)		
all (1451)	0.014 ± 0.001	0.014
intraresidue and sequential (699)	0.006 ± 0.003	0.005
short range (275)	0.014 ± 0.003	0.015
long range intramonomer (420)	0.016 ± 0.002	0.014
inter-monomer (48)	0.017 ± 0.003	0.015
hydrogen bonds (30)	0.029 ± 0.003	0.028
rmsd from experimental torsional angle restraints (deg)		
ϕ and ψ angles (56)	0.31 ± 0.06	0.25
CNX potential energies (kcal mol^{-1})		
E_{tot}	95.4 ± 7.3	87.2
E_{bond}	1.8 ± 0.6	1.5
E_{ang}	70.1 ± 2.9	67.9
E_{imp}	2.8 ± 0.2	2.5
E_{repel}	16.8 ± 2.0	13.8
E_{NOE}	2.5 ± 0.5	1.6
E_{cdih}	2.4 ± 0.3	0.01
E_{L-J}		−1276.3[d]
Cartesian coordinate rmsd (Å)	backbone	all heavy
$\langle SA \rangle$ versus $\overline{\langle SA \rangle}$[b] monomer	0.79 ± 0.13	1.14 ± 0.18
$\langle SA \rangle$ versus $\langle SA \rangle$[c] dimer	1.11 ± 0.23	1.32 ± 0.33
Procheck (*36*)		
residues in most favored and allowed regions		96%
residues in generously allowed regions		4%

[a] $\langle SA \rangle$ is the ensemble of the 10 lowest energy dimer structures, $\langle SA \rangle_{min}$ is the energy-minimized mean dimer structure. [b] For residues 6−117 of the survivin monomer. [c] For residues 6−117 of the survivin dimer. [d] E_{L-J} was not used in the refinement, but is included as an independent assessment of nonbonded geometry.

$^{15}N/^{13}C$ protein with an equal molar amount of unlabeled protein in the presence of 8 M urea and 50 μM $Zn(Ac)_2$. The mixture was left at room temperature for 2 days to allow the protein dimers to re-equilibrate. The protein was then slowly dialyzed to remove the urea. The folded protein was purified with a Superdex-75 gel filtration column. At equilibrium, fifty percent of the dimers contained in the final sample will be composed of an isotopically labeled and an unlabeled monomer.

Mature Smac/Diablo(56−239) was prepared by expressing the protein in *E. coli* BL21(DE3). A 6× histidine tag was added to the C-terminus and the protein was purified by Ni^{2+}-affinity chromatography.

NMR Spectroscopy. NMR samples contained 0.5−1.0 mM survivin protein in 50 mM phosphate (pH 7.5) and 1 mM [^{2}H]dithiothreitol. All NMR experiments were acquired at 298 K on a Bruker DRX500, DRX600 or DRX800 NMR spectrometer. Backbone ^{1}H, ^{13}C, and ^{15}N resonance assignments were obtained using a suite of deuterium-decoupled, triple-resonance experiments [HNCA, HN(CO)CA, HN(CA)CB, HN(COCA)CB, HNCO, and HN(CA)CO] (*19*−*21*). The side chain ^{1}H and ^{13}C NMR signals were assigned from H(CC−CO)NH, (H)C(C−CO)NH, or edited NOESY experiments. Stereospecific assignments for nine of the 11 leucine methyl groups were obtained from an analysis of the ^{13}C−^{13}C coupling patterns observed for biosynthetically directed, fractionally ^{13}C-labeled survivin (*22*). NOE distance restraints were obtained from three-dimensional ^{15}N- and ^{13}C-edited NOESY or three-dimensional ^{12}C-filtered ^{13}C-edited NOESY spectra acquired with a mixing time of 80 ms.

Structure Calculations. Monomer structures were calculated using a simulated annealing protocol with the program CNX (MSI, San Diego, CA) (*23*). Distance constraints between the zinc and the three chelated cysteins and one histidine of the BIR domain were included on the basis of earlier structural data (*15, 17*). Structures were calculated using 1394 intramonomer NOE constraints, 30 hydrogen-bond restraints derived from an analysis of amide exchange rates, and 56 torsional restraints from an analysis of the backbone chemical shifts (*24*) (Table 1). Dimer structures were calculated using an additional 48 intermonomer NOE constraints.

Low-energy monomer structures were docked to form the dimer and then refined using a simulated annealing protocol (*25, 26*). A square-well potential (F_{NOE} = 50 kcal mol^{-1}) was employed to constrain NOE-derived distances. There were no dihedral-angle violations greater than 5° and no NOE violations greater than 0.2 Å. Only covalent geometry, NOE, torsion, and repulsive terms were included in the structure refinement. Even so, the Lennard-Jones energy is large and negative, indicating that the structure has favorable nonbonded contacts.

Peptide Binding. Smac and peptide binding to survivin was assayed using [^{13}C,^{1}H]HSQC spectra on a selectively methyl (Leu, Val, and Ile-δ1) labeled sample (*27, 28*). Smac was titrated (12.5−200 μM) into a 25 μM survivin sample that was perdeuterated except for the methyl groups. Peak heights were measured at each concentration (*19*). Peak heights will be reduced as a resonance broadens. Resonances that broadened more rapidly than the average resonance are most likely due to direct contact with Smac/Diablo (*29*). Binding affinities of peptides [Ala-Val-Pro-Phe-Tyr, Abu-Val-Pro-Phe-Tyr, Ala-Tle-Pro-Phe-Tyr, Ala-Val-(N-Me)Ala-Phe-Tyr, Ala-Val-Pro-Tyr-Tyr, Ala-Val-Pro-Phg-Tyr, and Ala-Val-Pro-(Cl-Phe)-Tyr] were determined by titrating 12.5, 25, 50, 100, and 200 μM of the peptides into 25 μM survivin. The chemical shift perturbations for each ligand concentration are used to derive the K_d (*30*). To rank the binding of the remaining peptides, we used the protein chemical shift change (δ_{obs}) that occurred at 50 μM of ligand and the

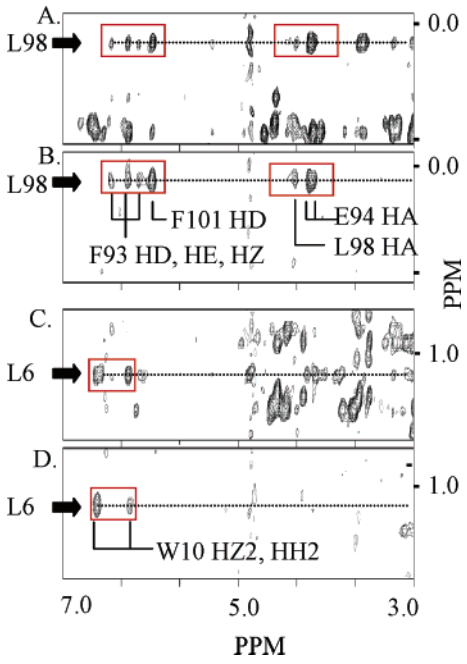

FIGURE 1: Representative NMR data defining dimer contacts. (A) Intra- and intermonomer NOE cross-peaks observed for L98 in a 3D ^{13}C-edited NOESY spectrum. (B) Intermonomer NOEs observed for L98 in 3D ^{12}C-filtered ^{13}C-edited NOESY spectrum. (C) Intra and intermonomer NOE cross-peaks observed for L6 in 3D ^{13}C-edited NOESY spectrum. (D) Intermonomer NOEs observed for L6 in 3D ^{12}C-filtered ^{13}C-edited NOESY spectrum. The peaks corresponding to the intermonomer NOEs are highlighted with red boxes.

average fully bound chemical shift change (δ_{sat}) derived from the previously mentioned six titrated peptides. The reported value was obtained from $K_d = (L^0 - P^0x)(1 - x)/x$ where $x = \delta_{obs}/\delta_{sat}$ and L^0 and P^0 are the added ligand and protein concentration. Peptides were synthesized in house.

RESULTS AND DISCUSSION

Defining the Dimer Interface of Survivin in Solution. The relevant dimer interface of human/mouse survivin is still controversial (*18*). To resolve this question, we determined the dimer interface of survivin observed in solution using high-resolution NMR spectroscopy. A sample containing a mixture of labeled (^{15}N,^{13}C) and unlabeled protein was prepared and used to define unambiguous contacts between the two monomers of survivin(1−120). The intermonomer contacts were determined using a ^{12}C-filtered ^{13}C-edited three-dimensional NOESY experiment (*31, 19*). This experiment selects for NOE contacts between an isotopically labeled and an unlabeled monomer. In Figure 1 are representative slices comparing the NOE data from a ^{13}C 3D-edited NOESY experiment (Figure 1A,C) to the data from a ^{12}C-filtered ^{13}C-edited 3D NOESY experiment (Figure 1B,D) (*19, 32*). Only NOE cross-peaks between a labeled and unlabeled monomer remain in the filtered NOESY slices (Figure 1B,D). Forty-eight intermolecular NOEs were observed between the monomers of the survivin dimer. These NOEs were all resolved from the diagonal in the 3D experiments. Additional NOE cross-peaks between degenerate resonances were observed on the diagonal in the ^{12}C-filtered ^{13}C-edited 3D NOESY experiment, but these contacts were not used as constraints in the structure calculations. Intermonomer NOEs were observed between the two central

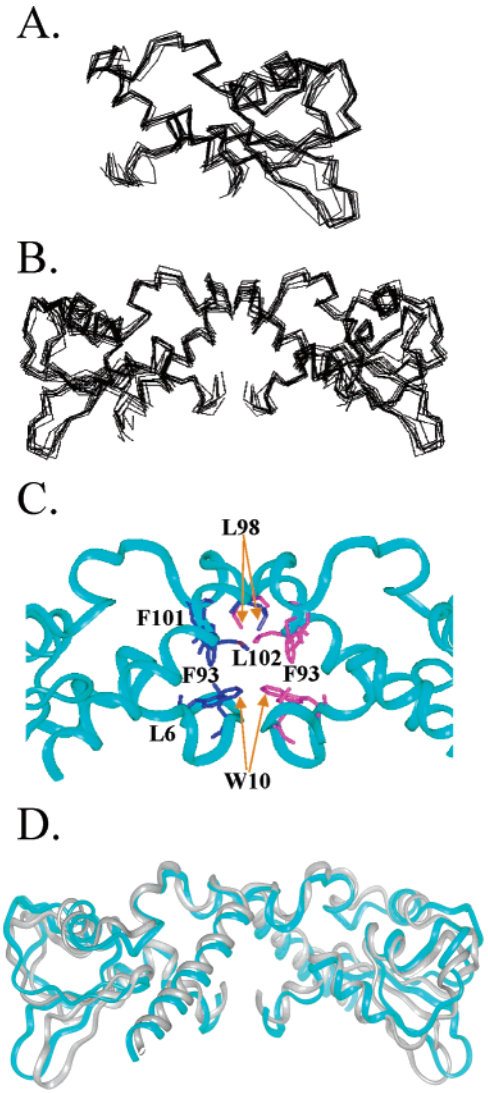

FIGURE 2: Structures of human survivin in solution. (A) View of 10 superimposed monomer NMR structures (residues 6−117). (B) View of 10 superimposed full survivin dimer NMR structures (residues 6−117). (C) Ribbon depiction of the average minimized solution NMR structure of the survivin dimer interface. Side chains of residues that have NOE contacts across the dimer interface are shown in magenta for one monomer and blue for the other monomer. (D) Ribbon depiction of a backbone superposition (residues 1−120) of the average minimized solution NMR structure (cyan) and the X-ray structures (gray) of human survivin (PDB 1F3H).

L98 residues of each monomer and the flanking residues L6, W10, F93, F101, and L102, which form the sides of a hydrophobic box around them. All of these observed contacts are consistent with the bow-tie-shaped dimer found earlier in the X-ray structures for human survivin (*15, 17*). No NOE contacts were observed between residues in the proposed zinc chelation dimer interface (*16*).

The structure of survivin in solution was determined from a total of 1394 intramonomer and forty-eight intermonomer NMR derived restraints. The structure of each survivin monomer was well-defined by the NMR data (Table 1, Figure 2A). The root-mean-square deviation (rmsd) to the mean coordinate position for residues 6−117 of each monomer is 0.79 ± 0.13 Å for backbone atoms and 1.14 ± 0.18 Å for all heavy atoms. The survivin dimer is also well-defined by the NMR data with an rmsd of 1.11 ± 0 0.23 Å

for the backbone atoms (Figure 2B). A ribbon representation of the average minimized survivin solution structure in the dimer interface is shown in Figure 2C. Side chains of residues that have NOE contacts across the dimer interface are also shown.

The structure of the survivin BIR domain consists of a three-stranded β-sheet and four α-helices. The solution and X-ray structures of the BIR domain monomers of survivin (6−90) are in very good agreement with an rmsd of 1.38 Å for the backbone atoms (Comparisons to PDB accession code 1F3H). In Figure 2D, we show a superposition of the NMR and the X-ray structure for the "bow-tie model" for the dimer of human survivin(1−120) (*15, 17*). The overall structures of the dimer are similar between the NMR and this X-ray structure with an rmsd of 1.2 Å in the dimer region (residues 6−13 and 89−105 for monomer A and B) and 1.9 Å for all backbone atoms (residues 6−105 for monomer A and B).

A notable feature of survivin among IAPs is the additional α-helix in the C-terminus. In this study we truncated the protein at residue 120 to improve the protein's solubility. This truncation removes part of the C-terminal α helix (Δ121−142). Our structural data indicate that truncation of survivin at residue 120 does not affect the structure of the BIR domain of the protein nor the ability of the protein to homodimerize in solution. Recently a splice variant of survivin has been reported that corresponds to the construct (residues 1−120) used in our studies (*33*). In addition, survivin(1−120) used in this study was able to interact with human aurora kinases with similar affinity as the full length protein, which indicates that this protein is folded and functional (*12*).

Survivin Binding to Smac/Diablo. Recently, survivin has been reported to interact with Smac/Diablo (*8*). To map the interface between survivin and Smac/Diablo, we performed NMR titrations of the two proteins. In these studies, we used an almost fully deuterated survivin(1−120) sample with only the methyl groups protonated and ^{13}C labeled (*28*) to improve the quality of the spectra. When mature Smac/Diablo (residues 56−239) is added to this sample, overall broadening of the spectrum was observed (Figure 3A), consistent with the increased size of the complex. Differential broadening between contact residues and those outside of the contact region is expected due to chemical exchange effects upon binding (*29*). As shown in Figure 3A,B, the methyl group of survivin with the greatest broadening upon addition of Smac/Diablo is residue L64. This additional broadening for L64 methyl groups is most likely due to chemical exchange broadening resulting from the direct contact of this residue with Smac/Diablo (*29*). In addition, L87, which is in the vicinity of L64, also shows above average broadening. Resonances that are distal to L64, like L14 or L98, which is in the dimer interface, exhibit much less broadening upon addition of Smac/Diablo (Figure 3B). Interestingly, L64 is in the proposed zinc chelation dimer interface in mouse survivin (*16*). Using the broadening data from the methyl resonances of L64, we estimate that the K_d for survivin/Smac/Diablo binding to be 22 μM. These data indicates that the binding is in fast exchange under the NMR sample conditions (*19*).

This binding data suggests that Smac/Diablo binds to a region of survivin that is homologous to the binding site for N-terminal Smac/Diablo peptides to BIR3 of XIAP. Residue

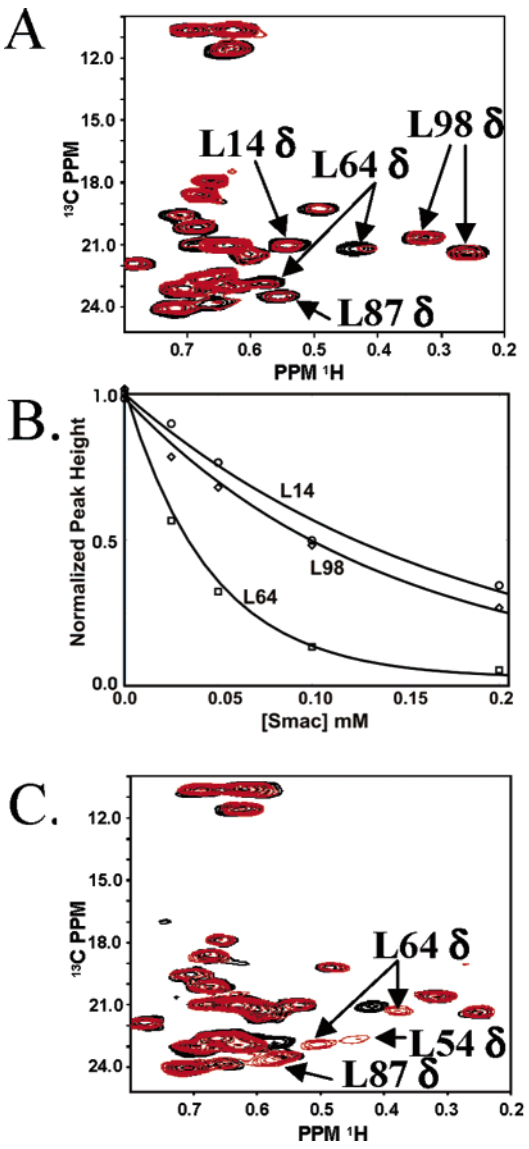

FIGURE 3: Broadening or chemical shifts changes of resonances of a selectively methyl (Leu, Val, and Ile-δ1) ^{13}C/^{1}H-labeled perdeuterated survivin. (A) [^{13}C,^{1}H]HSQC spectra after addition of 100 μM Smac/Diablo. (B) Height changes of representative methyl resonances of survivin as a function of added Smac/Diablo. (C) [^{13}C,^{1}H]HSQC spectra after addition of Hid peptide (AVPFY) (100 μM). In both parts A and C the reference spectra of the protein alone are black while the spectra after addition of titrant are red.

L64 of survivin corresponds to L307 in the BIR3 domain of XIAP, which sits in the center of the peptide binding pocket (*34*). Mutation of D71 in this site totally abolishes the interaction between survivin and Smac/Diablo (*8*). This mutation corresponds to the E314S mutation in the BIR3 domain of XIAP, which also abolishes binding to Smac/Diablo peptides (*34*). This site has already been implicated to be important for survivin's antiapoptotic activity. Mutations of residues H80 and E76 in this site in mouse survivin resulted in spontaneous apoptosis in HeLa cells (*16*).

Truncated forms of survivin with only the BIR domain (residues 1−99) have been reported not to interact with Smac/Diablo (*8*) or to localize to the mitotic spindle (*17*). To understand the role of the C-terminal helix for the function of survivin, we cloned and expressed the (residues 1−99) BIR domain only construct. [^{15}N,^{1}H]HSQC spectra for the (residues 1−99) construct did not have the same well-

Table 2: Binding Affinity of Peptides to Survivin and to the BIR3 Domain of XIAP[a]

	K_d (μM)			K_d (μM)			K_d (μM)			K_d (μM)	
position 1	**survivin**	**BIR3**	**position 2**	**survivin**	**BIR3**	**position 3**	**survivin**	**BIR3**	**position 4**	**survivin**	**BIR3**
Ala	**7**	0.06	**Val**	**7**	0.06	**Pro**	**7**	0.06	**Phe**	**7**	0.06
Me-Ala	13	0.04	**Tle**	**6**	0.04	Hyp	47	0.8	**Tyr**	**6**	0.3
Abu	**24**	0.04	Lys	17	0.05	Pip	60	0.4	**Cl-Phe**	**7**	0.18
Val	113	0.9	Phe	25	0.12	Sar	60	0.6	2-Na1	22	0.19
Nle	>200	>20	Abu	37	0.09	Aib	77	>20	**Phg**	**31**	0.03
D-Ala	>200	5	Leu	39	0.16	Gly	106	3	Val	32	0.9
Aib	>200	1.8	Nle	39	0.12	***N*-Me-Ala**	**134**	1.6	Cha	37	0.97
Me_2-Ala	>100	8.7	Ala	93	0.29	Aze	>200	0.12	Leu	44	0.28
Gly	>200	9.6	D-Ala	>200	>20				Ile	60	0.36
			D-Val	>200	>20				Nle	64	0.9
			D-Phe	>200	>20				1-Nal	77	0.09
			Aib	>200	>20				Homo-Phe	99	0.18
			Me-Ala	>200	>20				Gly	185	3.4
			Gly	>200	2.7				D-Phe	>200	0.8
									Aib	>200	6.7

[a] All the peptides were derived from the pentapeptide AVPFY. Four libraries were synthesized in which each of the first four residues was varied while keeping the other four residues unchanged. The binding affinity (K_d) against survivin was derived by NMR experiments as described in the Experimental Procedures. The binding affinity (K_d) against BIR3 was derived from a fluorescence polarization anisotropy (FPA) competition assay (*34*). The peptides' K_ds obtained from a five point NMR titration are highlighted in bold, the rest were obtained from the average saturating chemical shift and the chemical shift observed at a ligand concentration of (50 μM). All the amino acids have L-configuration unless indicated otherwise.

resolved resonances found for full length survivin or our survivin(1−120) construct (data not shown). The lack of well-resolved resonances is characteristic of unfolded or aggregated proteins. This result suggests that the (1−99) construct of survivin is not properly folded. This conclusion is consistent with the structure of the survivin dimer. In the structure, residues 99−110 are involved in making contacts across the dimer interface. These contacts are likely to be important for dimer formation and thus also for protein stability. Removing these key residues is likely to interfere with proper folding of the protein. All of the important dimer contacts are maintained in our (1−120) construct.

Survivin Binding to N-Terminal Peptides from Smac/Diablo. Smac/Diablo N-terminal peptide and its *Drosophila* homologues Hid and Grim have been shown to be able to bind to the BIR3 domain of XIAP with high affinity (*34*). We tested if the N-terminal peptides from Smac/Diablo (AVPIA), as well as the *Drosophila* homologues Hid (AVPFY) and Grim (AIAY) are also sufficient to bind tightly to survivin. We found that all three of these peptides bound weakly, with the Hid peptide (AVPFY) showing the best affinity of 7 μM. The peptide affinity we observe for (AVPIF) is similar to what we observed for full length Smac/Diablo, suggesting that most of the binding affinity comes from the N-terminal residues of Smac/Diablo. In Figure 3C, we show the chemical shifts changes observed when the Hid peptide is added to survivin. Similar to our earlier titration results with mature Smac/Diablo, the biggest resonance shifts are for the methyls of L64, L54, and L87. These titration data indicate that the N-terminal Smac/Diablo peptides also bind to the region around L64 of survivin.

To identify amino acid preferences for binding to survivin by N-terminal Smac/Diablo-like peptides, a library of pentapeptides was screened by NMR. Peptide binding to survivin was monitored using [^{13}C,^{1}H]HSQC spectra (*28*). In Table 2, we rank the binding affinity for each peptide in the library. As expected, the SAR (structure−activity relationships) for the peptides is similar to what was found earlier for peptide binding to the BIR3 domain (*34*, *35*). In the first position, Ala and Abu were tolerated, but larger (e.g. Nle) or smaller (e.g. Gly) amino acids resulted in a decrease in affinity. In addition, a positive charge at the N-terminus is required (*34*), as a methylamine was tolerated but a dimethylamine completely abrogated binding. No strong preference was found for position 2 of the peptide, while position 3 showed a preference for Pro. Finally, a Phe or large hydrophobic amino acid was preferred at the fourth position. Similar to the BIR3 domain, D-amino acids were not tolerated at any position. Strikingly, although the general trend in the SAR is similar for survivin and for the BIR3 domain of XIAP, no peptides could be identified that bound to survivin with an affinity better than 6 μM, while single-digit nanomolar peptides were identified for BIR3 of XIAP (Table 2) (*35*).

NOE studies were performed to define how one of these peptides, AKPFY, binds to survivin. NOEs observed between the AKPFY peptide and survivin, (e.g. K2'−E65, P3'−L64 and F4'−L54) indicate that the peptide binds across the third β-strand of survivin. In addition, residues W67 and E76 are broadened in the presence of the peptide. In Figure 4, we compare the structure of the survivin peptide binding site with the structure of the BIR3/AVPIA Smac/Diablo peptide complex (*34*). The survivin residues that have NOEs to or are broadened by the peptide are shown in Figure 4B. These contacts are consistent with a peptide binding mode similar to that found for the BIR3 domain. Furthermore, the NOE data indicates that the AKPFY peptide binds across the third β-strand of survivin in the same orientation as the AVPIA peptide binds to the BIR3 domain (*33*).

Although the binding mode for peptides is similar to BIR3, differences in the residues of the survivin peptide binding pocket may significantly reduce peptide binding. For example, in the BIR3/AVPIA peptide complex, the carbonyl group of the first residue of the peptide is in position to hydrogen bond with the indole of W323. This is likely to be an important contact, since in BIR3 a W323A mutation reduces binding of the Smac peptide by more than 50-fold (*34*). In survivin, a histidine (H80) replaces the tryptophan (W323) found in BIR3 (Figure 4B). This may contribute to

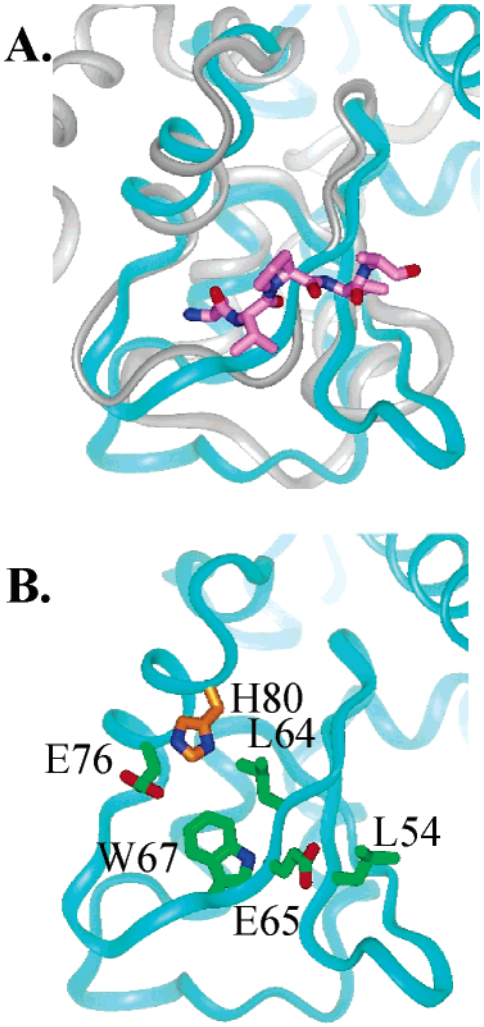

FIGURE 4: Smac/Diablo N-terminal peptide binding pocket of survivin. (A) Superposition of the ribbon representation of a survivin monomer (cyan) and the BIR3 (gray)/AVPIA Smac peptide complex (*34*). The AVPIA peptide is shown in magenta. (B) Same view of survivin showing the side chains (green) of residues in the survivin/AKPFY complex that have NOEs to the peptide or are broadened by its presence. H80 of survivin is colored brown.

the more than 100-fold loss in affinity of Smac/Diablo-derived peptides for survivin when compared to the BIR3 domain of XIAP.

CONCLUSIONS

Survivin is involved in both cell cycle regulation and apoptosis (*1*, *2*). It is overexpressed in most human cancers and represents an attractive target for cancer therapy. We have determined the dimer interface of human survivin that is found in solution. These data clearly resolves the controversy concerning the relevant dimer interface of human/mouse survivin (*18*). We have also demonstrated that a truncated construct of survivin(1−120) containing the BIR domain and part of the last helix folds correctly and is sufficient to bind Smac/Diablo. Finally, we have provided data that indicate how human survivin interacts with Smac/Diablo. Residues that are involved in the binding interaction are localized to a region near β3 and α4 of survivin and the binding of N-terminal Smac/Diablo-like peptides are consistent with the binding mode observed earlier for peptide binding to the XIAP BIR3 domain.

ACKNOWLEDGMENT

The authors would like to thank Binu Issac, Jun Chen, and Danying Song for assistance and Philip Hajduk, Liping Yu, and Jonathan Greer for helpful comments on the manuscript.

SUPPORTING INFORMATION AVAILABLE

Stereoviews of the NMR-derived structure of survivin and comparisons to an X-ray structure of both survivin (PDB ID 1F3H) and BIR3 Smac/Diablo peptide complex (PDB ID 1G3F), a FPA titration curve for peptide binding to BIR3, ^{13}C HSQC of survivin before and after preparation of the mixed labeled homodimer, a table summarizing the experimental NMR collection parameters, and a table of peptide binding constants with error bars. This material is available free of charge via the Internet at http://pubs.acs.org.

REFERENCES

1. Altieri, D. C. (2003) Survivin, versatile modulation of cell division and apoptosis in cancer, *Oncogene 22*, 8581−8589.
2. Altieri, D. C. (2003) Validating survivin as a cancer therapeutic target, *Nat. Rev. Cancer 3*, 46−54.
3. Salvesen, G. S., and Duckett, C. S. (2002) IAP proteins: Blocking the road to death's door, *Nat. Rev. Mol. Cell Biol. 3*, 401−410.
4. Fesik, S. W., and Shi, Y. G. (2001) Structural biology—Controlling the caspases, *Science 294*, 1477−1478.
5. Shi, Y. G. (2002) Mechanisms of caspase activation and inhibition during apoptosis, *Mol. Cell 9*, 459−470.
6. Blanc Brude, O. P., Mesri, M., Wall, N. R., Plescia, J., Dohi, T., and Altieri, D. C. (2003) Therapeutic targeting of the survivin pathway in cancer: Initiation of mitochondrial apoptosis and suppression of tumor-associated angiogenesis, *Clin. Cancer Res. 9*, 2683−2692.
7. Marusawa, H., Matsuzawa, S., Welsh, K., Zou, H., Armstrong, R., Tamm, I., and Reed, J. C. (2003) HBXIP functions as a cofactor of survivin in apoptosis suppression, *EMBO J. 22*, 2729−2740.
8. Song, Z. Y., Yao, X. B., and Wu, M. (2003) Direct interaction between survivin and Smac/DIABLO is essential for the anti-apoptotic activity of survivin during taxol-induced apoptosis, *J. Biol. Chem 278*, 23130−23140.
9. Adams, R. R., Carmena, M., and Earnshaw, W. C. (2001) Chromosomal passengers and the (aurora) ABCs of mitosis, *Trends Cell Biol. 11*, 49−54.
10. Reed, J. C., and Bischoff, J. R. (2000) BIRinging chromosomes through cell division − And survivin′ the experience, *Cell 102*, 545−548.
11. Wheatley, S. P., Carvalho, A., Vagnarelli, P., and Earnshaw, W. C. (2001) INCENP is required for proper targeting of Survivin to the centromeres and the anaphase spindle during mitosis, *Curr. Biol. 11*, 886−890.
12. Chen, J., Jin, S., Tahir, S. K., Zhang, H. C., Liu, X. S., Sarthy, A. V., McGonigal, T. P., Liu, Z. H., Rosenberg, S. H., and Ng, S. C. (2003) Survivin enhances Aurora-B kinase activity and localizes Aurora-B in human cells, *J. Biol. Chem. 278*, 486-490.
13. Sun, C., Cai, M., Gunasekera, A. H., Meadows, R. P., Wang, H., Chen, J., Zhang, H., Wu, W., Xu, N., Ng, S. C., and Fesik, S. W. (1999) NMR structure and mutagenesis of the inhibitor-of-apoptosis protein XIAP, *Nature 401*, 818−822.
14. Sun, C., Cai, M., Meadows, R. P., Xu, N., Gunasekera, A. H., Herrmann, J., Wu, J. C., and Fesik, S. W. (2000) NMR structure and mutagenesis of the third Bir domain of the inhibitor of apoptosis protein XIAP, *J. Biol. Chem. 275*, 33777−33781.
15. Chantalat, L., Skoufias, D. A., Kleman, J. P., Jung, B., Dideberg, O., and Margolis, R. L. (2000) Crystal structure of human survivin reveals a bow tie-shaped dimer with two unusual alpha-helical extensions, *Mol. Cell 6*, 183−189.
16. Muchmore, S. W., Chen, J., Jakob, C., Zakula, D., Matayoshi, E. D., Wu, W., Zhang, H. C., Li, F. Z., Ng, S. C., and Altieri, D. C. (2000) Crystal structure and mutagenic analysis of the inhibitor-of-apoptosis protein survivin, *Mol. Cell 6*, 173−182.

17. Verdecia, M. A., Huang, H. K., Dutil, E., Kaiser, D. A., Hunter, T., and Noel, J. P. (2000) Structure of the human anti-apoptotic protein survivin reveals a dimeric arrangement, *Nat. Struct. Biol. 7*, 602−608.
18. Shi, Y. G. (2000) Survivin structure: crystal unclear, *Nat. Struct. Biol. 7*, 620−623.
19. Cavanagh, J., Fairbrother, W. J., Palmer, A. G., and Skelton, N. J. (1996) *Protein NMR spectroscopy. Principles and practice*, Academic Press, Inc., San Diego, CA.
20. Clore, G. M., and Gronenborn, A. M. (1998) NMR structure determination of proteins and protein complexes larger than 20 kda, *Curr. Opin. Chem. Biol. 2*, 564−570.
21. Yamazaki, T., Lee, W., Arrowsmith, C. H., Muhandiram, D. R., and Kay, L. E. (1994) A suite of triple resonance NMR experiments for the backbone assignment of ^{15}N, ^{13}C, ^{2}H labeled proteins with high sensitivity, *J. Am. Chem. Soc. 116*, 11655−11666.
22. Neri, D., Szyperski, T., Otting, G., Senn, H., and Wuthrich, K. (1989) Stereospecific NMR assignment of Val and Leu *Biochemistry 28*, 7510−7516.
23. Brunger, A. T. (1992) *X-PLOR Version 3.1*, Yale University Press, New Haven.
24. Cornilescu, G., Delaglio, F., and Bax, A. (1999) Protein backbone angle restraints from searching a database for chemical shift and sequence homology, *J. Biomol. NMR 13*, 289−302.
25. Nilges, M. (1993) A calculation strategy for the structure determination of symmetric dimers by ^{1}H NMR, *Proteins 17*, 297−309.
26. ODonoghue, S. I., King, G. F., and Nilges, M. (1996) Calculation of symmetric multimer structures from NMR data using a priori knowledge of the monomer structure, comonomer restraints, and interface mapping: The case of leucine zippers, *J. Biomol. NMR 8*, 193−206.
27. Goto, N. K., Gardner, K. H., Mueller, G. A., Willis, R. C., and Kay, L. E. (1999) A robust and cost-effective method for the production of Val, Leu, Ile methyl-protonated N-15-, C-13-, H-2-labeled proteins., *J. Biomol. NMR 13(4)*, 369−374.
28. Hajduk, P. J., Augeri, D. J., Mack, J., Mendoza, R., Yang, J. G., Betz, S. F., and Fesik, S. W. (2000) NMR-based screening of proteins containing C-13-labeled methyl groups, *J. Am. Chem. Soc. 122*, 7898−7904.
29. Matsuo, H., Walters, K. J., Teruya, K., Tanaka, T., Gassner, G. T., Lippard, S. J., Kyogoku, Y., and Wagner, G. (1999) Identification by NMR spectroscopy of residues at contact surfaces in large, slowly exchanging macromolecular complexes, *J. Am. Chem. Soc. 121*, 9903−9904.
30. Wang, Z.-X. (1995) An exact mathematical expression for describing competitive binding of two different ligands to a protein, *FEBS Lett. 360*, 111−114.
31. Breeze, A. L. (2000) Isotope-filtered NMR methods for the study of biomolecular structure and interactions, *Prog. Nucl. Magn. Reson. Spectrosc. 36*, 323−372.
32. Fesik, S. W., and Zuiderweg, E. R. P. (1988) Heteronuclear Three-Dimensional NMR SPectroscopy. A Strategy for the Simplification of Homonuclear Two-Dimensional NMR Spectra, *J. Magn. Reson. 78*, 588−593.
33. Badran, A., Yoshida, A., Ishikawa, K., Goi, T., Yamaguchi, A., Ueda, T., and Inuzuka, M. (2004) Identification of a novel splice variant of the human anti-apoptosis gene survivin, *Biochem. Biophys. Res. Commun. 314*, 902−907.
34. Liu, Z., Sun, C., Olejniczak, E. T., Meadows, R. P., Betz, S. F., Oost, T., Herrmann, J., Wu, J. C., and Fesik, S. W. (2000) Structural basis for binding of Smac/DIABLO to the XIAP BIR3 domain, *Nature. 408*, 1004−1005.
35. Oost, T. K., Sun, C., Armstrong, R. C., Al-Assaad, A. S., Betz, S. F., Deckwerth, T. L., Ding, H., Elmore, S. W., Meadows, R. P., Olejniczak, E. T., Oleksijew, A., Oltersdorf, T., Rosenberg, S. H., Shoemaker, A. R., Tomaselli, K. J., Zou, H., and Fesik, S. W. (2004) Discovery of potent antagonists of the anti-apoptotic protein XIAP for the treatment of cancer, *J. Med. Chem. 47*, 4417−4426.
36. Laskowski, R. A., MacArthur, M. W., Moss, D. S., and Thornton, J. M. (1993) Procheck, *J. Appl. Crystallogr. 26*, 283−291.

BI0485171